Journal of Alloys and Compounds 509S (2011) S612–S615

Contents lists available at ScienceDirect

Journal of Alloys and Compounds

journal homepage: www.elsevier.com/locate/jallcom

Atomization energy approach to the quantitative evaluation of catalytic activities of metal oxides during dehydrogenation of MgH_2

H. Hirate [a,*], M. Morinaga [a], H. Yukawa [a], H. Nakai [b]

[a] Department of Materials Science and Engineering, Graduate School of Engineering, Nagoya University, Furo-Cho, Chikusa-Ku, Nagoya 464-8603, Japan
[b] Department of Chemistry and Biochemistry, School of Advanced Science and Engineering, Waseda University, Okubo, Shinjuku-ku, Tokyo, 169-8555, Japan

ARTICLE INFO

Article history:
Received 16 July 2010
Received in revised form 4 October 2010
Accepted 6 October 2010
Available online 14 October 2010

Keywords:
Hydrogen storage
MgH_2
Quantitative evaluation
$NaAlH_4$
Atomization energy

ABSTRACT

The hydrogen desorption reaction of magnesium hydride (MgH_2), $MgH_2 \rightarrow Mg + H_2$, is accelerated by mixing catalytic metal oxides (e.g., Nb_2O_5). This catalytic effect is evaluated quantitatively using the atomization energy concept. The measured hydrogen desorption rate increases monotonously with increasing $y \times \Delta E_O$ values of metal oxides, M_xO_y. Here, $\Delta E_{O,}$ is the atomization energy for the oxide ion in M_xO_y. This indicates that the oxide ion interacts mainly with hydrogen atom in MgH_2, in agreement with the observation of the O–H stretching mode in the FT-IR spectra during the dehydrogenation of the Nb_2O_5-catalyzed MgH_2. This approach is also proved to be useful for the catalytic analysis of metal chlorides (e.g., $TiCl_3$) on the decomposition reaction of $NaAlH_4$ expressed as, $NaAlH_4 \rightarrow (1/3)Na_3AlH_6 + (2/3)Al + H_2$

1. Introduction

Magnesium hydride (MgH_2) is one of the promising candidates for hydrogen storage, because it possesses a high hydrogen capacity of 7.6 wt.% [1,2]. In 1999, Liang et al. reported that some metal could act as a catalyst to enhance the hydrogen absorption and desorption reactions [3]. Also, it was found that transition metal oxides (e.g., Nb_2O_5) have a large catalytic effect on the hydrogen desorption reaction of MgH_2 [4–7]. However, no quantitative approach has been proposed yet.

Recently, Nakai proposed a new analyzing method of the total energy called energy density analysis (EDA) [8]. In this method, the total energy of a system, computed by the Kohn-Sham-type density functional theory (DFT) [9], is partitioned into atomic energy densities. We have applied this method to the analysis of the chemical bond between atoms in various hydrides and hydrocarbons [10–12]. In this analysis, the atomization energy for each constituent atom is newly defined by subtracting the atomic energy density from the total energy of the isolated atom. This energetic analysis allows us to compare the nature of the chemical bond between atoms among a variety of materials in a quantitative way.

Recently, catalytic activities of metal oxides for the hydrogen desorption reaction of MgH_2 have been evaluated quantitatively using the atomization energy concept [13]. In this paper, we review our previous works. Special attention is directed toward the experimental verification of the concept through the FT-IR spectroscopic observation of the O–H bond during the dehydrogenation of Nb_2O_5-catalyzed MgH_2 [14]. The atomization energy concept is further applied to the decomposition reaction of $NaAlH_4$ with metal chloride catalysts [15].

2. Calculation and experimental procedure

2.1. Energy density analysis (EDA)

The electronic structures for metal oxides and metal chlorides are obtained by the DFT calculations under the periodic boundary condition (PBC) using Gaussian03 program package (Gaussian, Inc., Wallingford, CT). The adopted functional is the BLYP functional [16]. The EDA calculations under PBC [17] are performed by linking the original code for the EDA with Gaussian03. The modified Gaussian basis sets and calculation details are referred to [13,15].

2.2. Atomization energy

The EDA analysis is performed with the crystal geometry optimized by the plane-wave pseudopotential method [8]. For binary metal oxides, M_xO_y, the respective atomic energy densities of M and O are related closely to the nature of the chemical bond relevant to M and O atoms in M_xO_y. When the energy of the isolated neutral atom, E_M^{atom} (or E_O^{atom}), is taken as a reference, the atomization energy, ΔE_M (or ΔE_O), is defined as,

$$\Delta E_M = (E_M^{atom} - E_M^{oxide}) \times \left(\frac{x}{y}\right) \quad (1)$$

$$\Delta E_O = E_O^{atom} - E_O^{oxide} \quad (2)$$

where E_M^{oxide} and E_O^{oxide} are the atomic energy densities for M and O in M_xO_y, respectively. In the above equation (1), a coefficient, (x/y), is multiplied to $(E_M^{atom} - E_M^{oxide})$, so this ΔE_M is the average energy of M to be counted per oxide ion.

---

[*] Corresponding author.
E-mail address: hirate@silky.numse.nagoya-u.ac.jp (H. Hirate).

0925-8388/$ – see front matter © 2010 Published by Elsevier B.V.
doi:10.1016/j.jallcom.2010.10.013

Table 1
Calculated and experimental cohesive energies for metal oxides (units: eV).

	E_{coh}(Calc.)	E_{coh}(Exp.)		E_{coh}(Calc.)	E_{coh}(Exp.)
Al_2O_3	10.67	10.59	Cr_2O_3	9.19	9.27
SiO_2	9.49	9.63	NbO	15.35	14.38
TiO_2	10.23	9.92	NbO_2	10.14	10.51
V_2O_5	8.44	7.94	Nb_2O_5	9.31	9.56

Then, the cohesive energy, E_{coh}, of the oxide per oxide ion is defined as,

$$E_{coh} = \Delta E_M + \Delta E_O \quad (3)$$

Thus, ΔE_M and ΔE_O are the components of E_{coh}. Each of the atomization energies become a measure of the chemical bonding effect of the element on the stability of the metal oxides.

Similarly, for binary metal chlorides, MCl_n, the atomization energy per chloride ion, ΔE_M (or ΔE_{Cl}), is defined as,

$$\Delta E_M = \frac{(E_M^{atom} - E_M^{chloride})}{n} \quad (4)$$

$$\Delta E_{Cl} = E_{Cl}^{atom} - E_{Cl}^{chloride} \quad (5)$$

2.3. Synthesis and dehydrogenation of Nb_2O_5-catalyzed MgH_2

Powders of MgH_2 (98%) and Nb_2O_5 (99.99%) are purchased from Sigma-Aldrich Inc. MgH_2 specimens with and without 1 mol% Nb_2O_5 catalyst are milled for 20 h at 400 rpm under a hydrogen pressure of 1 MPa at ambient temperature using a planetary ball mill apparatus (Firitsch P7).

All the specimens are always handled in an argon-filled glove box equipped with a recirculation system to keep the water and oxygen concentrations below 1 ppm during operation.

Four specimens are made from milled MgH_2 with 1 mol% Nb_2O_5 and used for the FT-IR measurements; (a) specimen released no hydrogen (called non-released specimen), (b) released hydrogen about 2.3 wt.% (2.3 wt.% released specimen), (c) released hydrogen about 5.6 wt.% (5.6 wt.% released specimen), and (d) released hydrogen completely (all-released specimen). Here, hydrogen is released from the specimen by heating at 573K in vacuum for an appropriate time in a Sievert-type apparatus following a standard volumetric method.

2.4. FT-IR measurements

A standard technique is employed for the measurement of FT-IR spectroscopy. With the specimens prepared as potassium bromide (KBr) pellets, FT-IR spectra are measured in the range of 800–4000 cm^{-1} at room temperature in vacuum, using JASCO FT/IR-610 instrument.

3. Results

3.1. Cohesive energy for binary metal oxides

The cohesive energy, E_{coh}, is a measure of the electronic stability of any oxides. As shown in Table 1, the difference between the calculated and experimental values [18] for E_{coh} lies within 0.5 eV, except for NbO [19]. Thus, the present calculation is performed in a reasonable manner.

3.2. Atomization energy diagram for binary metal oxides

The plots of ΔE_M vs. ΔE_O, are shown in Fig. 1 for binary metal oxides, M_xO_y. This ΔE_M vs. ΔE_O diagram is called "atomization energy diagram". The contribution of each element in the oxide to the cohesive energy is understood from this figure, following Eq. (3). For example, the cohesive energy is nearly same between NbO_2 and Al_2O_3. However, they are located in the very different positions in Fig. 1. NbO_2 has a large ΔE_O value, but a very small ΔE_M value, indicating that the oxide ions in NbO_2 make a significant contribution to the cohesive energy. On the contrary, in case of Al_2O_3, the value of ΔE_O is almost zero, but instead ΔE_M is very large. In this way, using the atomization energy diagram, the roles of each constituent element in the stability of metal oxides can be understood in a straightforward manner. Such information is, however, never obtained from the total energy calculation alone.

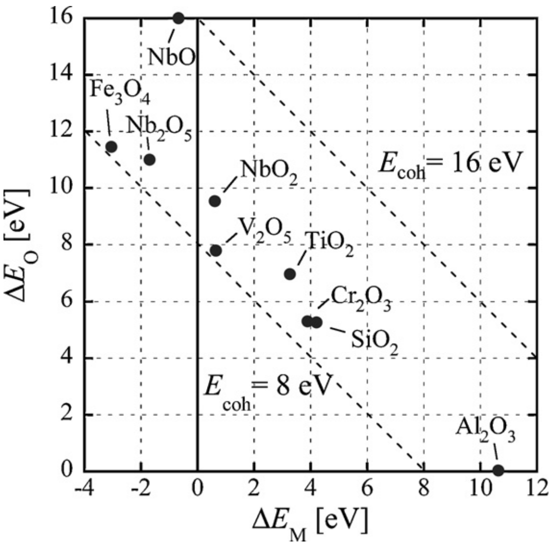

Fig. 1. Atomization energy diagram for metal oxide catalysts.

3.3. Quantitative analysis of catalytic activities of metal oxides for MgH_2

As a measure of the catalytic activity of each metal oxide, the measured hydrogen desorption rate is adopted [13]. The values reported by Barkhordarian et al. [7] are listed in Table 2.

To evaluate the catalytic activity quantitatively, the atomization energies of constituent elements in metal oxides are used. As is evident from Eqs. (1) and (2), atomization energies are defined as the values per oxide ion. However, metal oxides, M_xO_y, are mixed by a mole unit in the experiment. So, the values of the atomization energies are needed to be converted into the values per mole unit. Therefore, each of ΔE_O and ΔE_M is multiplied by the number of oxide ions, y, in M_xO_y, that is expressed as $y \times \Delta E_O \ \ (= (E_O^{atom} - E_O^{oxide}) \times y)$, and $y \times \Delta E_M \ \ (= (E_M^{atom} - E_M^{oxide}) \times x)$.

The measured desorption rate is plotted against the atomization energy for oxide ions, $y \times \Delta E_O$, or metal ions, $y \times \Delta E_M$, as shown in Fig. 2(a) and (b). The result shown in Fig. 2(a) indicates that metal oxides which have large $y \times \Delta E_O$ values tend to accelerate hydrogen desorption rate of MgH_2. On the other hand, the result shown in Fig. 2(b) is the reverse of this trend, since metal oxides which have small $y \times \Delta E_M$ values tend to accelerate hydrogen desorption rate.

In our previous study on the hydrogenation process of TiFe or Mg_2Ni, it is shown that that the element (e.g., Fe or Ni) with the higher atomization energy interacts more strongly with hydrogen atom than the element (e.g., Ti or Mg) with the lower atomization energy [11]. As a result, hydrogen atoms are located near Fe in $TiFeH_2$, and near Ni in Mg_2NiH_4. Thus, the element with the higher atomization energy in the metal oxide must interact more strongly with hydrogen atom in MgH_2. In other words, the oxide ions in the metal oxides with larger $y \times \Delta E_O$ values are supposed to interact more strongly with hydrogen atoms in MgH_2, as is shown in Fig. 2(a).

Table 2
Various metal oxides and their catalytic effect on hydrogen desorption reaction rate of MgH_2 at 573 K.

	Desorption rate [$\times 10^{-2}$%/s]		Desorption rate [$\times 10^{-2}$%/s]
Nb_2O_5	10.2	Cr_2O_3	1.9
V_2O_5	6.0	TiO_2	1.9
NbO_2	3.5	Al_2O_3	0.7
NbO	2.0	SiO_2	0.2

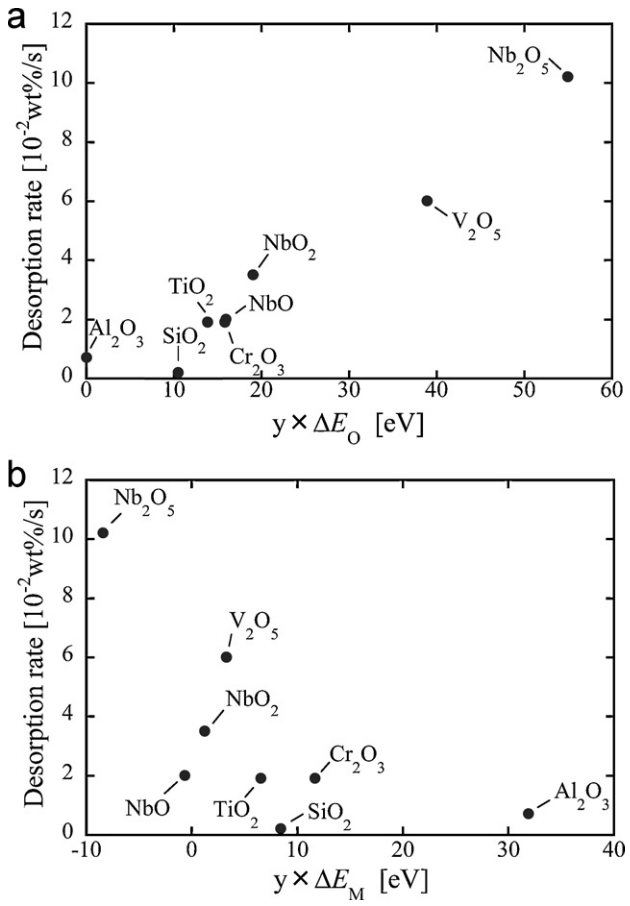

Fig. 2. (a) $y \times \Delta E_O$, (b) $y \times \Delta E_M$ vs. desorption rate of MgH_2 with 1 mol% metal oxide catalysts at 573 K.

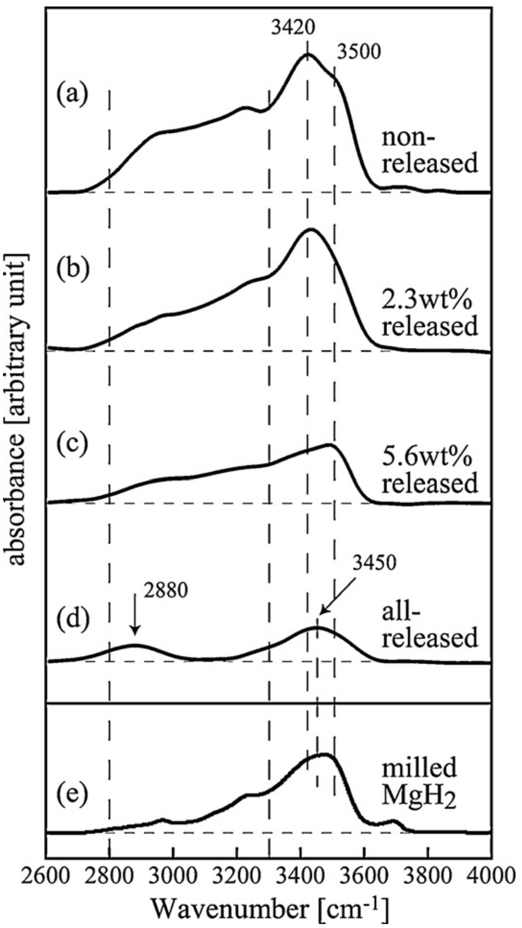

Fig. 3. FT-IR spectra of MgH_2 with 1 mol% Nb_2O_5 in the region of 2600–4000 cm^{-1}, (a) non-released, (b) 2.3 wt.% released, (c) 5.6 wt.% released, (d) all-released specimen and (e) milled MgH_2 for comparison.

3.4. O–H bonding during the course of dehydrogenation reaction of Nb_2O_5-catalyzed MgH_2

From the atomization energy concept, it is predicted that the oxide ions in metal oxides interact with hydrogen atoms in MgH_2 during the dehydrogenation of MgH_2. So, an experiment is performed to observe this O-H interaction between O ions in metal oxide and H atoms in MgH_2 using FT-IR spectroscopy [14].

According to previous experiments, the O–H bonding in the absorbed hydroxyl group appears in the region of 3000–3800 cm^{-1} due to the O–H stretching mode [20–23]. So, the FT-IR spectra are measured in the region of 2600–4000 cm^{-1}, as shown in Fig. 3.

As is evident from Fig. 3(a), there are two bands at 3420 and 3500 cm^{-1}, and a broad band from 2800 to 3300 cm^{-1} in the spectrum from the non-released specimen. The absorption intensities decrease gradually with decreasing amount of hydrogen retained in the specimen, as shown in Fig. 3(a)–(c). However, as shown in Fig. 3(d), two small bands at 2880 and 3450 cm^{-1} are still observed in the all-released specimen, despite that no MgH_2 remains in it, judging from the non-appearance of any peaks from MgH_2 in the XRD profile. In addition, as shown in Fig. 3(e), several bands appear in the milled MgH_2, although the intensities are weaker compared to those of the non-released specimen shown in Fig. 3(a). The band at 3450 cm^{-1} is also observed in the all-released specimen as shown in Fig. 3(d). So, this may be related partially to the existence of MgO, since it is observed in both the milled MgH_2 and all-released specimens. Some O-H vibrations might retain on the surface of MgO, but the detail still remains unknown.

It is confirmed from the present experiment that the O-H interaction between Nb_2O_5 and MgH_2 is operating during the course of dehydrogenation reaction of Nb_2O_5-catalyzed MgH_2. Therefore, the atomization energy of oxide ion, ΔE_O, in metal oxide catalysts is indeed a good measure of the catalytic activities in the dehydrogenation reaction of MgH_2.

3.5. Quantitative evaluation of catalytic activities of metal chlorides for $NaAlH_4$

The atomization energy concept is further applied to the catalytic reaction problem of $NaAlH_4$ [15]. It is well known that the decomposition reaction of $NaAlH_4$ is accelerated by mixing metal chloride catalyst (e.g., $TiCl_3$). In analogy with the desorption reaction of MgH_2 with metal oxide catalysts, the catalytic activities of each metal chloride are evaluated using the decomposition reaction rate of $NaAlH_4$ [24].

The atomization energies of constituent elements in metal chlorides are used to understand catalytic activities of metal chlorides, and the results are shown in Fig. 4(a) and (b). Each value of $n \times \Delta E_M$ and $n \times \Delta E_{Cl}$ is the atomization energy counted per mole unit derived from Eqs. (4) and (5).

Following the multi-regression analysis [15], metal chlorides which have large values of $n \times \Delta E_M$ are supposed to accelerate the rate of the decomposition reaction from $NaAlH_4$ to Na_3AlH_6, as shown in Fig. 4(a). For example, in case of $TiCl_3$ or $TiCl_4$, Ti works probably as a more active element than Cl in the catalytic reaction.

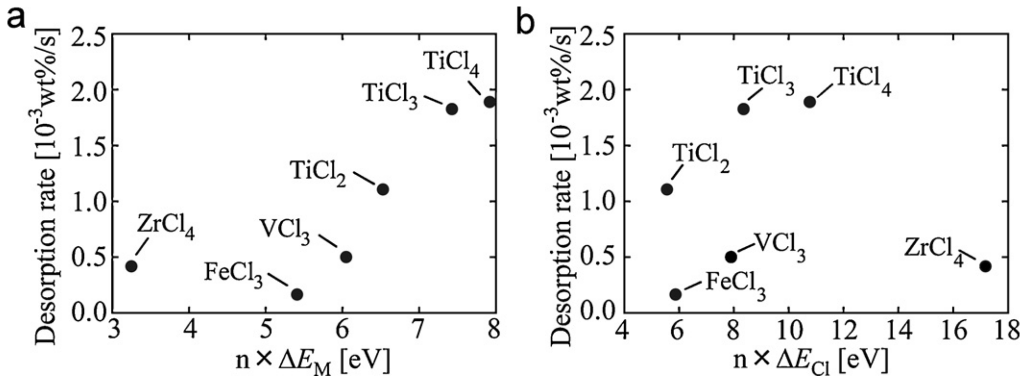

Fig. 4. (a) $n \times \Delta E_M$, (b) $n \times \Delta E_{Cl}$ vs. desorption rate of $NaAlH_4$ with 2 mol% metal chloride catalysts at 393 K.

4. Summary

New atomization energy concept is applied for the first time to the practical problems on the hydrogen desorption reaction of MgH_2 with the metal oxide catalysts and also on the decomposition reaction of $NaAlH_4$, with the metal chloride catalysts. It is shown that the oxide ions in the metal oxides, M_xO_y with larger $y \times \Delta E_O$ values interact more strongly with hydrogen atoms in MgH_2. This is confirmed experimentally through the observation of the O-H stretching mode in the FT-IR spectra during the dehydrogenation of the Nb_2O_5-catalyzed MgH_2. Also, metal chlorides, MCl_n which have large values of $n \times \Delta E_M$, tend to accelerate the decomposition reaction of $NaAlH_4$.

This concept will be applicable to most of the problems on catalytic reactions. Thus, the present approach will give a new clue to the design of new catalysts in a variety of chemical reactions.

Acknowledgment

This study was supported by a Grant-in-Aid for Scientific Research from the Japan Society for the Promotion of Science.

References

[1] J.F. Stampfer Jr., C.E. Holley Jr., J.F. Suttle, J. Am. Chem. Soc. 82 (1960) 3504–3508.
[2] D.L. Cummings, G.J. Powers, Ind. Eng. Chem. Process Des. Dev. 13 (1974) 182–192.
[3] G. Liang, J. Huot, S. Boily, A. Van Neste, R. Schulz, J. Alloys Compd. 292 (1999) 247–252.
[4] W. Oelerich, T. Klassem, R. Bormann, J. Alloys Compd. 315 (2001) 237–242.
[5] G. Barkhordarian, T. Klassen, R. Bormann, Scr. Mater. 49 (2003) 213–217.
[6] G. Barkhordarian, T. Klassen, R. Bormann, J. Alloys Compd. 364 (2004) 242–246.
[7] G. Barkhordarian, T. Klassen, R. Bormann, J. Phys. Chem. B 110 (2006) 11020–11024.
[8] H. Nakai, Chem. Phys. Lett. 363 (2002) 73–79.
[9] W. Kohn, L.J. Sham, Phys. Rev. 140 (1965) A1133–1138.
[10] Y. Shinzato, H. Yukawa, M. Morinaga, T. Baba, H. Nakai, J. Alloys Compd. 446 (2007) 96–100.
[11] Y. Shinzato, H. Yukawa, M. Morinaga, T. Baba, H. Nakai, Acta Mater. 55 (2007) 6673–6680.
[12] Y. Shinzato, H. Yukawa, M. Morinaga, T. Baba, H. Nakai, Adv. Quant. Chem. 54 (2008) 145–160.
[13] H. Hirate, Y. Saito, I. Nakaya, H. Sawai, Y. Shinzato, H. Yukawa, M. Morinaga, T. Baba, H. Nakai, Int. J. Quant. Chem. 109 (2009) 2793–2800.
[14] H. Hirate, H. Sawai, H. Yukawa, M. Morinaga, Int. J. Quant. Chem., in press, doi:10.1002/qua.22544.
[15] H. Hirate, Y. Saito, I. Nakaya, H. Sawai, Y. Shinzato, H. Yukawa, M. Morinaga, T. Baba, H. Nakai, Int. J. Quant. Chem., in press, doi:10.1002/qua.22459.
[16] J.C. Slater, Phys. Rev. 81 (1951) 385–390.
[17] H. Nakai, Y. Kurabayashi, M. Katouda, T. Atsumi, Chem. Phys. Lett. 438 (2007) 132–138.
[18] R.C. Weast, M.J. Astle, W.H. Beyer, CRC Handbook of Chemistry and Physics: A Ready-Reference Book of Chemical and Physical Data, 84th ed., CRC Press, Boca Raton, 2003.
[19] A.L. Bowman, T.C. Wallace, J.L. Yarnell, R.G. Wenzel, Acta Crystallogr. 21 (1966), 843–843.
[20] G. Busca, Catal. Today 41 (1998) 191–206.
[21] L.J. Burcham, J. Datka, I.E. Wachs, J. Phys. Chem. B 103 (1999) 6015–6024.
[22] T. Armaroli, G. Busca, C. Carlini, M. Giuttari, A.M.R. Galletti, G. Sbrana, J. Mol. Catal. A: Chem. 151 (2000) 233–243.
[23] V.S. Braga, J.A. Dias, S.C.L. Dias, J.L. de Macedo, Chem. Mater. 17 (2005) 690–695.
[24] D.L. Anton, J. Alloys Compd. 356–357 (2003) 400–404.